 doi:10.20944/preprints202108.0157.v1

Ventricular septation and outflow tract development in crocodilians result in two aortas with bicuspid semilunar valves

Robert E. Poelmann[1,2], Adriana C. Gittenberger-de Groot*, Charissa Goerdajal[1], Nimrat Grewal[3] , Merijn A.G. De Bakker[1], Michael K. Richardson[1]

[1]Dept of Animal Sciences and Health, Institute of Biology, Sylvius Laboratory, University of Leiden, Sylviusweg 72, 2333BE, Leiden, The Netherlands.

[2]Dept of Cardiology, Leiden University Medical Center, Albinusdreef 2, P.O.box 9600, 2300RC Leiden, The Netherlands.

[3]Dept of Cardiothoracic Surgery, Leiden University Medical Center, Albinusdreef 2, P.O.box 9600, 2300RC Leiden, The Netherlands.

Dedicated to the memory of Adriana C. Gittenberger-de Groot whose ideas were instrumental in this research project.

Key words:

reptile, ventricular septation, endocardial cushions, semilunar valves, outflow tract, cartilage, foramen of Panizza, left aorta, right aorta, pulmonary trunk, pharyngeal arch arteries, coronary arteries.

 doi:10.20944/preprints202108.0157.v1

Abstract

Background. The outflow tract of crocodilians resembles that of birds and mammals as ventricular septation is complete. The arterial anatomy however, presents with a pulmonary trunk originating from the right ventricular cavum, and two aortae originating from either the right or left ventricular cavum. Mixing of blood in crocodilians cannot occur at ventricular level as in other reptiles, but instead takes place at aortic root level by a shunt, the Foramen of Panizza, the opening of which is guarded by two facing semilunar leaflets of both bicuspid aortic valves.

Methods. Developmental stages of *Alligator mississipiensis, Crocodilus niloticus* and *Caiman latirostris*, have been studied.

Results and Conclusions. The outflow tract septation complex can be divided into 2 components. The aorto-pulmonary septum divides the pulmonary trunk from both aortae, whereas the interaortic septum divides the systemic from the visceral aorta. Neural crest cells are most likely involved in the formation of both components. Remodeling of the endocardial cushions and both septa results in the formation of bicuspid valves in all three arterial trunks. The foramen of Panizza originates intracardially as a channel in the septal endocardial cushion.

Preprints (www.preprints.org) | NOT PEER-REVIEWED | Posted: 6 August 2021 doi:10.20944/preprints202108.0157.v1

Introduction.

The bicuspid aortic valve (BAV) is the most common congenital cardiac malformation in humans with a frequency of 0.5-2 % [1]. Furthermore, the malformation is associated with aortic aneurysm in 60-80% of the BAV-population later in life [2] and is, therefore, of clinical importance [3]. Much is known about the embryonic origin of abnormal leaflet numbers associated with genetic mutations in the human population [3a], but also in genetic models of mice such as GATA5 [4], Krox20 [5], Notch [6], aggrecan [7], periostin [8],nitric oxide synthase [9], in hamsters [10] and also in bird hemodynamics [8, 11]. It is evident that several cell populations act in concert during the formation of the semilunar valves. These include the endocardial cushions, neural crest cells and second heart field. Less is known about the development of the arterial valves in reptiles where bicuspidy is the rule [12, 13]. Our restricted level of knowledge is comprehensible as a lack of marker experiments is hampering cell lineage research in the reptilian setting, while genetic mutants affecting specifically outflow tract development have not been published to our knowledge. This does not mean that tools are unavailable. In an evolutionary context the comparison of development may elucidate the characteristics of bicuspidy in different taxa. Here, we report the development of the arterial valves in three species of crocodilians (*Crocodylus niloticus, Alligator mississipiensis and Caiman latirostris*) to be discussed against mammalian and avian backgrounds. The remodeling of the endocardial cushions will be investigated during outflow tract septation, leading to the separation of three main arteries. These are the pulmonary trunk and left-sided aorta both emerging from the right ventricle, and the right-sided aorta emerging from the left ventricle. All three arteries contain bicuspid valve leaflets. Finally, the septal outflow tract cushion (in crocodilians only) is further specialized. Here, we find the origin of two septal components involved in the separation of the three main arterial stems and furthermore, the intracardiac origin of a channel between the left and right-sided circulation, i.e. both aortas. After separation and remodeling of the outflow tract this shunt, known as the Foramen of Panizza, (first described by the Italian anatomist Bartolomeo Panizza, 1785-1867 [14, 15] connects

Preprints (www.preprints.org) | NOT PEER-REVIEWED | Posted: 6 August 2021 doi:10.20944/preprints202108.0157.v1

the roots of the left and right aorta that in specific circumstances may convey blood from the right ventricle to the main circulation [16-18] and sometimes vice versa.

General description.

In crocodilians the presence of 3 interconnected ventricular cava, as common in reptiles, is apparent in early stages. However, during the development described here, this distinction becomes lost because interventricular septation takes place and the resulting division is conveniently described as left and right ventricle. This comes with a consequence as in crocodilians 2 aortas persist (as in other reptiles), each deriving from one of those ventricles. To avoid complications related to left/right sidedness in the body and right/left origin of the respective aortas, we have chosen to use the term "systemic aorta" (sAo) for the morphologically right-sided aorta that derives from the left ventricle, while "visceral Aorta" (vAo) denominates the left-sided aorta that branches from the right ventricle (similarly as used in Poelmann [19]. Note: Cook et al [20] countered the sidedness problem differently by employing the terms 'left-ventricular aorta' and 'right-ventricular aorta', respectively). Our choice is further substantiated by the observation that the right ventricle perfuses both the abdominal and thoracic viscera as the left-sided aorta (->vAo) will perfuse the intestines or viscera (Axelsson 1991) and the right-sided pulmonary blood will perfuse the lungs (note that viscera and lungs are both 'endoderm-derived' organ systems), whereas the left ventricle and right-sided aortic blood (->sAo) will mostly perfuse the combination of body wall, extremities and head/neck region.

List of abbreviations

AP *Aorto-Pulmonary septum;* ***Apc*** *Aortic parietal cushion;* ***AV*** *atrioventricular cushion;* ***ca*** *carotid artery;* ***dAo*** *dorsal Aorta;* ***FS*** *folding septum;* ***ggl*** *ganglion;* ***IA*** *Inter-Aortic septum;* ***IS*** *inflow septum;* ***LA*** *left atrium;* ***LV*** *left ventricle;* ***LVOT*** *left ventricular outflow tract;* ***MB*** *main bronchi;* ***ms*** *membranous septum between LV and RV;* ***myo*** *myocardium;* ***Oes*** *oesophagus;* ***p*** *foramen of Panizza;* ***Ppc*** *pulmonary parietal cushion;* ***Pu*** *pulmonary trunk;* ***RA*** *right atrium;* ***RV*** *right ventricle;* ***RVOT*** *right ventricular outflow tract;* ***sAo*** *systemic Aorta;* ***sc*** *septal cushion;* ***SV*** *sinus of Valsalva;* ***T*** *trachea;* ***vAo***

Preprints (www.preprints.org) | NOT PEER-REVIEWED | Posted: 6 August 2021 doi:10.20944/preprints202108.0157.v1

*visceral Aorta; # ventral myocardium, part of AP septum; * (presumably) left-sided neural crest cells, part of AP septum; + (presumably) right-sided neural crest, part of IA septum; Δ dorsal myocardium, part of AP septum.*

Description of stages

Ferguson stage 17. The right and left ventricle are dorsally intersected by the Inlet septum (Fig 1 a) , but otherwise not separated, as the interventricular communication presents itself clearly (Fig 1b). The ventricular inlet septum is fused with the large central AV-cushion complex, while the folding septum [19] can hardly be discerned (Fig 1a-c). Slightly more downstream the septal outflow tract cushion (sc) becomes apparent, together with the flanking aortic and pulmonary parietal outflow tract cushions (Apc and Ppc) (fig 1d-f). In the septal cushion two streaks of condensed mesenchymal cells are evident, one on the pulmonary side (red curve in Fig 1g-i), the other on the aortic side (blue curve). At their tips (* and + in Fig h, i) both contain a histologically very dense cluster of cells. The pulmonary streak or Aorto-pulmonary (AP) septum, might contain left-sided NC derived cells, while the aortic streak or Interaortic (IA) septum, contains probably right-sided NC cells . The curved lumen of the outflow tract (Fig 1h, i) can be divided into the pulmonary outflow tract (from the right ventricle), the visceral aorta (vAo, also from the right ventricle) and the systemic aorta (sAo, left ventricle). Separation of the outflow tracts (Fig 1j) takes place by 1. the AP septum including a ventral myocardial spur (# in Fig1 j- n) located between the pulmonary trunk and the aortas, 2. by the IA septum between sAo and vAo. In the thorax no further branches will be found emanating from the vAo. The sAo however branches further in both carotid arteries (not depicted here).

Ferguson stage 19. The interventricular situation (Fig 2a, b) has not advanced very much compared to stage 17 as the interventricular communication is still open and the folding septum (FS) remains inconspicuous, yet (Fig 2c). The septal outflow tract cushion (sc) acquires a dense core (Fig 2c)

Preprints (www.preprints.org) | NOT PEER-REVIEWED | Posted: 6 August 2021 doi:10.20944/preprints202108.0157.v1

preceding the differentiation of cartilage in next the stage. The interconnected lumina of the LVOT and RVOT are easily recognized (Fig 2d, e) interrupted by the large septal cushion (sc). The root of the Pu seems to be connected sideways (Fig 2d-f) to the ventricular segment as a result of folding of this part of the interventricular septum. The septal cushion is located at the top of the folding septum (Fig 2 c, d) that becomes more clear in the next stage. In the as yet common outflow tract the three arteries become separated by the AP septum and the IA septum. In the AP septum the region of the originally dense cluster of cells (see Fig 2 h *) surrounds a dorsal spur of myocardium (Δ in Fig 2 g, h) being the cranial tip of the folding septum. This dorsal myocardial spur has not fused yet with the ventral myocardial spur (# Fig 2j-m and dashed red line (Fig l) to show the continuation with the ventral wall) as there is a 'window', free from myocardium in between (* in Fig2 h-j). AP separation and IA separation are seemingly spatially independent from each other (Fig2 i, j). The septal cushion is distally completely bisected by the AP-septum (Fig 2k). The right-sided IA-septum deviates between both aortae with a dense cell cluster at its tip (+ in Fig 2h, i)

The transition of the cardiac tube to the arterial vascular wall deserves special attention. It is evident that the arterial wall extends inside the cardiac tube over a considerable distance estimated to be about 200 µm on the pulmonary side and even about 400 µm on the aortic side (white dashed line in Fig 2k). Downstream this appearance is even more substantiated (Fig 2m), where nearly the complete ventral wall of the vAo seems to consist of a double layer of vessel wall and myocardium (white dashed line) with hardly a thin endocardial cushion tissue. This continues to an estimated depth of 350-400 µm into the myocardial tube. As a consequence we are dealing with 2 concentric tubes, a myocardial circumference surrounding an arterial wall.

Ferguson stage 20. The interventricular communication between LVOT and RV is almost closed (Fig a). The dense core in the septal and in the aortic parietal cushions start to differentiate into cartilage as seen by intense Alcian blue staining (Fig 3 a-c), although more downstream this differentiation is not apparent, yet (Fig d, e). Here, the IA septum consists of densely packed right-sided neural crest

Preprints (www.preprints.org) | NOT PEER-REVIEWED | Posted: 6 August 2021 doi:10.20944/preprints202108.0157.v1

cells as described in the earlier stages (+ in Fig 3d). The AP septum now contains a clear core of myocardium (**Δ** in Fig 3d-f) as part of the incurving dorsal wall of the myocardial tube. Where the septal cushion has connected with the ventral wall also the ventral myocardial spur (# in Fig 3f-h) is present. The 2 spurs do not contact each other (* depicts the mesenchymal 'window' between the myocardial spurs indicated by **Δ** and # in Fig 3 g). The AP and IA septum deviate (Fig 3h, i) to continue outside the heart as the mesenchymal vessel walls of the respective arteries. (Fig 3j-l). The common stem of the carotid arteries (ca) branches from the systemic aorta (Fig 3l). Two sinus of Valsalva (white arrow) are present in the OFT cushions of the systemic aorta and the pulmonary trunk (Fig 3h,i) as the first sign of the forming semilunar valve leaflets. The situation in the visceral aorta is slightly different as in the parietal cushion a sinus of Valsalva is still lacking, but in the septal cushion a very narrow slit is seen representing the sinus of Valsalva that is connected to the main lumen of the vAo, being probably the first sign of the origin of the Foramen of Panizza (see description in the next stage 21).

Ferguson stage 21 . The ventricular inflow septum (IS) is seen as the continuation of the folding septum (Fig a, b), beyond the topping cartilage of the septal cushion (Fig 4 b-e). Another, smaller, piece of cartilage is found in the aortic parietal cushion (Fig 4c, d). In the outflow tract the pulmonary side becomes separated from the aortic side by the large septal cushion, containing the elements of the AP septum (* and Δ in Fig4 e-h) as well as the IA septum (+ in Fig 4f-h). Here, an interesting feature becomes apparent known as the Foramen of Panizza (FOP, black arrows in Fig 4f, g), connecting the 2 septal sinus of Valsalva of the sAo(white arrow) and vAo. Actually, the FOP in this stadium is a very narrow channel, about 100 µm high in cranio-caudal direction and about 200 µm between both sinus. The channel surrounds the advancing tip of the IA (+ in Fig 4f, g) that at this level is completed in arterial direction only (Fig 4h, i). Further downstream the myocardial tube is replaced by the arterial vessel walls in the concentric manner described above. The stem of the carotid arteries branches from the sAo (Fig 4 j, k).

Preprints (www.preprints.org) | NOT PEER-REVIEWED | Posted: 6 August 2021 doi:10.20944/preprints202108.0157.v1

Ferguson stage 22 . Most of the features described for stage 21 apply for this stage. The folding septum is more advanced (Fig 5a). The condensed mesenchyme in the septal cushion is further differentiated into cartilage (Fig 5 b-d) even reaching to the level of the FOP (Fig 5d, e, black arrows). The FOP is seen as a very narrow channel rounding the cartilaginous tip at the base of the IA (Fig 5d, e). The condensed mesenchyme in the aortic parietal cushion is advanced and now contains 2 cartilaginous centers (Fig 5c), one in the continuation of the aortic vessel wall and a second one in the cushion mesenchyme. The ventral and dorsal myocardial spurs (# and Δ in Fig 5e) have joined with no mesenchymal window anymore in between, implying that a small myocardial bridge has been established in the AP septum. The IA septum does not acquire a myocardial component in contrast to the AP septum (Fig 5e-g). The branching of the main arterial stems is demonstrated in Fig 5 h-i. The pulmonary trunk is divided into the 6th left and right pulmonary arch arteries (PAA6, 5Fig h), the vAo, being the left 4th PAA, does not branch further, whereas the stem of the carotid arch arteries splits from the right 4th PAA being the sAo (Fig5 h-i).

Ferguson stage 24. The folding and the inlet septum are meeting each other at an angle with the septal outflow tract cushion as hinge (Fig 6a, b). The inlet septum continues between the LVOT and the right ventricle (Fig 6b, c) while the septal and aortic parietal cushions have fused over a short distance (Fig 6d) to reopen again further downstream. A mesenchymal interventricular septum is not apparent, yet in contrast to stage 25. The IA septum is likewise not fully developed, leaving a lumen contact between sAo and vAo (Fig 6 e, f). Both imply that left-right separation has not been established, yet. The cartilage prongs are well-differentiated both in the septal cushion and aortic parietal cushion, in the latter 2 cartilage elements are present (Fig 6e, f) as in earlier stages. The FOP in the septal cushion is wide open connecting both the vAo's and sAo's sinus of Valsalva (Fig 6f-i). Further downstream the septal cartilage partly penetrates the interaortic septum (Fig 6j). In the root

Preprints (www.preprints.org) | NOT PEER-REVIEWED | Posted: 6 August 2021 doi:10.20944/preprints202108.0157.v1

of the sAo the double orifice of the coronary artery is present (orange arrow in Fig 6k, l), splitting immediately in a descendent and a circumflex branch (Fig 6l).

Ferguson stage 25. The spongious myocardium of the left and right ventricles have increased considerably in mass (Fig 7a, b). The cartilage of the septal outflow tract cushion is embedded deep apically between the left and right ventricle squeezed between the inlet and folding segments (Fig 7a). The presence of the mesenchymal septum (even better visible in the next stage) between left and right ventricle shows that complete septation has taken place. Even in this stage the complete separation of the sAo and vAo by the interaortic septum has not been established as there is a narrow lumen contact seen between LVOT and RVOT (Fig 7 b-h) and as a consequence also between (left-ventricular) sAo and (right-ventricular) vAo. This implies a complete interventricular septation from now on, but for the narrow connection between sAo and vAo provided by the FOP (black arrows in Fig 7 e-g) and the narrow lumen contact between both aortas. Functionally, in this embryo the FOP is closed as no red blood cells are found trapped in its lumen. The vAo appears very compressed in this particular embryo (Fig 7i).

Beyond Ferguson stage 25 (Alligator). In this HE stained series the LV and RV are completely septated and the hallmark of this process is the mesenchymal septum extending over a considerable distance (Fig 8a-d), reaching as far as the IA septum (Fig 8d, e). In the outflow tract the septal cushion is penetrated by the FOP (black arrow), connecting both septal sinus of Valsalva of the sAo and the vAo (Fig 8e, f) at the level where the arterial wall is inserted into the myocardium. Slightly more downstream the IA septum separates the two aortas whereas the AP septum completely separates the pulmonary trunk from the vAo (Fig 8g, h). Note that Fig 8h is alcian blue stained to demonstrate the myocardium versus the mesenchymal wall of the arteries.

Discussion

Preprints (www.preprints.org) | NOT PEER-REVIEWED | Posted: 6 August 2021 doi:10.20944/preprints202108.0157.v1

The endocardial cushions.

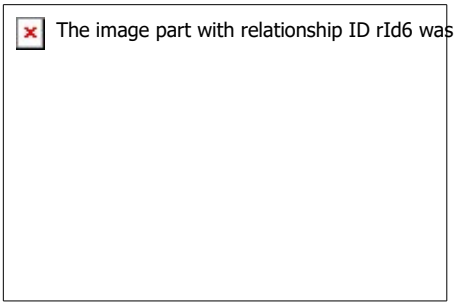

More than a century ago Hochstetter [12] provided a description of crocodilian heart development. He numbered 4 outflow tract endocardial cushions, Hochstetter's #1 being the septal cushion as described here. The # 2, 3, and 4 appeared as separate cushions in each of the 3 main arteries, which we took together as the parietal cushion, as early in development these combine as one cushion. Only during separation this cushion becomes divided over the sAo, the vAo and the pulmonary trunk. Furthermore, Hochstetter already discerns the 'septum aortico pulmonale' and the 'septum aorticum'. In his textfigures 10 and 13 he describes in *Crocodilus madasgacariensis* (first described in [22] which is probably an eastern divergent from *C. niloticus*, [23] the separation of both aortas to occur *before* that of the AP septum. Even in our youngest stage the AP and IA septum are found in the same embryo albeit at different levels. Apparently, the exact timing of these events is not strictly orchestrated. This heterochrony may indicate that the different cellular players are relatively independent from each other in the formation of the individual septum components.

Outflow tract separation

We decided that early in development two OFT cushion complexes could be discerned, the dorsal-most septal cushion and the more ventrally located parietal cushion. The single septal cushion (Sc) hugs the folding septum, the latter might also be called the vertical or muscular septum [12, 24] and is positioned between the left and right outflow tracts. The OFT cushions start with endocardial-mesenchymal transition of the lining endocardium, but become subsequently invaded by 'condensed mesenchyme' as shown in this study and also in birds [25], in human [26] and turtles [19]. The cellular origin in chicken and mouse is established to derive from the cardiac neural crest as demonstrated with various marker studies [27-31] The mesenchyme of the two main semilunar valve leaflets derives likewise from the cardiac neural crest, while the second heart field, important for

Preprints (www.preprints.org) | NOT PEER-REVIEWED | Posted: 6 August 2021 doi:10.20944/preprints202108.0157.v1

development of the right side of the heart including the pulmonary trunk [32, 33] participates in the development of the third, so-called non-facing semilunar valve leaflet as shown by the expression of Cardiac Troponin T2 [34, 35] or NKx2.5 [31]. Furthermore, a part of the septation complex does not derive from the cardiac crest [36] This is demonstrated in quail-chicken chimeras [25] in which a narrow zone of compact chick mesenchyme remains present in an otherwise quail-dominated septation complex. This narrow strip is also recognized between the two advancing myocardial components in the conal septum of our caiman AP-septum (depicted by * in Figs 1i, 2h, 3f etc..).

The neural crest cells migrate into the septal cushion from cranial and dorsal positions [28, 29, 31, 37], meeting the most cranial extension of the folding septum. Sumida [38] investigated the contribution of the left- and right-sided neural crest separately by transplanting quail crest isotopically and unilaterally into chicken host. They observed only ipsilateral NC contribution to the pharyngeal arch arteries and to the OFT endocardial cushions, with limited crossing to the contralateral side of the AP septum. The columns of condensed mesenchyme in the OFT cushions were derived from both sides of the NC in a complementary fashion, whereas the septal cartilage presented only right-sided NC cells. Likewise, left and right-sided columns of NC cells converging on the OFT septal complex are observed in the mouse (Peterson et al 2018) after immunostaining for AP2α, a marker of neural crest cells. These studies demonstrate the existence of separate streams of NC cells, and in crocodilians we show that these streams do not mix (red and blue in fig 1 and 2 g-j). The left-sided stream is at the base of the AP septum and the right-sided stream forms the IA septum.

This process is correlated to the persistence of two aortas in reptiles. In birds only the right aortic arch artery persists after pharyngeal arch remodeling, whereas in mammals the left one persists and the right one is further downstream incorporated into the subclavian artery. The left stream of condensed mesenchyme stays in close proximity to the folding septum and grows out to form part of the AP septum. The right stream deviates at almost 90 degrees to initiate the IA septum. The septal

Preprints (www.preprints.org) | NOT PEER-REVIEWED | Posted: 6 August 2021 doi:10.20944/preprints202108.0157.v1

cushion becomes divided into 3 entities, each dedicated to one of the 3 main arterial trunks as result from ingrowth of the two streams of condensed mesenchyme. Lineage tracing experiments in mouse and chicken have established that in these species the single AP septal complex derives particularly from the cardiac neural crest. In the next chapter we argue that the participation of second heart field cells in septation is restricted.

In older stages the parietal cushions present with two long legs, the aortic (Apc) and pulmonary parietal cushion (Ppc) along the right and left ventricular OFT. Only upon aortic separation (in Ferguson stage 20 and beyond) the Apc divides into 2 bulges dedicated to one of the aortic channels each. It is noteworthy to mention that the pulmonary parietal cushion is not involved in the separation process, but only in formation of a semilunar valve leaflet.

Cartilage in the OFT cushions.

A prominent developmental step in crocodiles starting in the most proximal tip of the condensed mesenchyme is the differentiation into cartilage. This is already noted deep in the ventricle in Ferguson stage 20 and occurs in both the Sc and the Apc. It increases in length and diameter and becomes a dominant feature in the distal OFT. At the base of the Sc close to the folding septum the differentiation process of cartilage increases dramatically. The non-cartilaginous condensed mesenchyme of the IA inside the Sc protrudes towards the Apc eventually establishing contact of the Sc with the Apc. The Apc in stage 22 and more pronouncedly differentiated in stage 24 carries even a double center of cartilage. At this point we need to address the question about the origin of the IA and the cartilage prongs. As described above a *bona fide* lineage marker is not available, therefore we have to rely on circumstantial evidence to discuss the participation of neural crest and second heart field-derived cells. In various chicken [25, 27, 38] and mouse [31, 39] models the contribution of neural crest cells to the OFT-septal complex has been proven unequivocally. Interestingly, in a neural crest-specific overexpression mouse model of TGFβ1 the OFT septum differentiates into

Preprints (www.preprints.org) | NOT PEER-REVIEWED | Posted: 6 August 2021 doi:10.20944/preprints202108.0157.v1

cartilage, demonstrating that cardiac NC cells are capable of differentiation into cartilage [40]. In neural crest quail/chicken chimera cartilage was a product of transplanted quail cells differentiating at the time of hatching [38]. Neural crest cells occupy the inner media of the aorta in an adult Wnt1-Cre mouse model, these derive from the embryonic complete media. Taken together, we postulate that the IA derives from the cardiac NC. A consequence is that the wall of the systemic aorta, being continuous with the IA, originates likewise from the NC [33, 41]. The origin of the wall of the visceral aorta is not completely deducted by this reasoning. It can be argued that in the side facing the systemic aorta also NC-derived cells are present as both aortae share the IA septum. The opposite side of the visceral aorta, however, is shared with the pulmonary trunk with the joining AP-septum in between. In mice [33, 36, 42, 43] it is known that the root of the pulmonary trunk is of mixed (NCC and SHF) origin. The OFT septal complex in mouse (Peterson 2018) and chicken [25, 27, 29, 44], that we consider here as a fusion product of the crocodilian IA plus AP septum, derives mainly from the cardiac NC. At this point it is important to evaluate again the paper of Sumida (1989) in which quail chicken chimeras were made of the right or left halve of the neural crest. These authors showed that a right and a left NC stream converged upon the chicken OFT-septal complex, but remained separate in the condensed mesenchyme. In particular in our *Caiman* material two streams of condensed mesenchyme (Fig 2g-j) are present each addressing only one of the septa involved. Furthermore, the stream in blue entered both the septal and parietal cushions (Sumida 1989) and is, therefore, responsible for cartilage formation in both cushions. In an earlier paper [19] we showed that the aortic and pulmonary flow dividers contain NC and second heart field cells in varying degrees and assumed that the IA septum might originate from the second heart field, and the AP septum from neural crest. With the currently available material we propose that the core of both septal components derives from the cardiac neural crest.

Cardiac cartilage is encountered in the chicken [38] and in specific groups of mammals such as hamsters [45]. In adult otters [46] and various ungulates such as buffalo [47], white rhinoceros [48] and sheep [49], a 'heart bone' is present in the fibrous trigone between left AV canal and aorta. A

Preprints (www.preprints.org) | NOT PEER-REVIEWED | Posted: 6 August 2021 doi:10.20944/preprints202108.0157.v1

subgroup of diseased chimpanzees with myocardial fibrosis presented with trabecular bone or hyaline cartilage in the right fibrous trigone [50]. In (sub)adult alligators a cartilage crown is present nearly completely encircling the roots of both aortas [20, 51]), but penetrating not as deep into the ventricle as described by us. In our embryonic crocodiles, alligators and caimans the cartilage elements have not fused, which was also the case in one juvenile crocodile of approximately 60 cm overall length. Other reptiles [52], terrapin ([53, 54], and turtle [19] present with cartilage prongs. We hypothesize that the elements being aorta-bound, most likely develop from the left NC stream. Evidently, the NC condensed mesenchyme and ensuing cartilage is encased by fibroblasts (Figure) and the origin of these fibroblasts needs further investigation. To our knowledge second heart field-derived cells do not have the capacity to differentiate into cartilage and neither do cultured pericardial cells [55]. In addition, fibroblasts or smooth muscle cells are found inside the myocardial OFT tube as an extension of the arterial walls (see Fig 3k, dashed line), the origin of which is also not clarified. We suggested earlier [19] that the aortic and pulmonary flow dividers, in which second heart field-derived cells also play a role [37], might be involved. Without proper markers, however, the participation of NCC and SHF derived cells (see fig 1 g, h) remains an educated guess even when more or less related species are considered for comparison. With respect to the other potentially involved cell populations such as the second heart field and epicardial/pericardial cells, further research is warranted.

Bicuspid semilunar valves

In mammals and birds tricuspid semilunar valves are the rule, while in reptiles bicuspid valves are consistently present. Mammalian bicuspidy is considered a congenital malformation [35] that is often associated with a fragile wall of the ascending aorta later in life [56]. Therefore, we need to find an explanation for the bicuspid valve in our crocodilians associated with a healthy aortic wall. In development the emerging OFT cushions present as the septal and parietal cushion. During

Preprints (www.preprints.org) | NOT PEER-REVIEWED | Posted: 6 August 2021 doi:10.20944/preprints202108.0157.v1

development these reach from a deep intraventricular position adjacent to the atrioventricular cushions distally towards the arterial pole. At the arterial pole the septal cushion, harboring the Anlage of the IA and the AP septum, becomes divided in 3 subcushions protruding in each arterial stem being the pulmonary trunk, the visceral aorta and the systemic aorta. The outgrowing interaortic septum eventually meets the aortic parietal cushion separating this cushion in 2 subcushions. The pulmonary parietal cushion develops singly as it is not continuous anymore with the Apc. Finally, every artery contains 2 cushions, one derived from the septal cushion and one from the subdivided parietal cushion. Specifically in the visceral aorta a small Ap-cushion remnant remains after the fusion process that could be compared to an intercalated cushion. However, this does not develop into a semilunar valve leaflet, probably because this remnant will not be filled by second heart field derived cells as is normally the case in e.g. mice (Peterson 2018). We know from chicken and mouse studies that the 2 main cushions are filled by mesenchymal cells derived both by epithelium-mesenchymal transition from the endocardium, as well as by later arriving neural crest cells. The third leaflet has a second heart field related etiology as demonstrated in a mouse NOS3 -/- model for bicuspidy [31]. In view of the human fragile aortic wall it is probably this third/non-coronary valve leaflet's etiology that associates with the differentiation of the outer media of the aortic wall, and that becomes prone to aneurysm formation. The inner media of the wall of the ascending aorta is NC derived[41, 57], whereas the outer media/adventita is SHF derived [5, 36]. We postulate that anomalous SHF differentiation may affect both this semilunar valve leaflet and the integrity of the ascending aorta.

Foramen of Panizza

Unique to crocodilian hearts is the foramen of Panizza [19, 20, 51, 58]. This is a tunnel inside the septal cushion that penetrates the IA septum, providing a seemingly intracardiac shunt between the right and left circulations. Here, it is assumed that the matrix of the OFT endocardial cushions is produced by cardiomyocytes similarly to the origin of the AV-cushions [59, 60]. This does not mean

Preprints (www.preprints.org) | NOT PEER-REVIEWED | Posted: 6 August 2021 doi:10.20944/preprints202108.0157.v1

that the whole OFT cushion remains within the myocardial border. The proximal part stays intramyocardially while the distal part extends without doubt into the arterial tube at the level of the semilunar valve leaflets. Consequentially, the fully grown location of the FOP being enclosed in the distal part of the septal cushion, is located outside the heart, connecting the facing sinus of Valsalva between the roots of both aortae. This has implications on the way we envisage semilunar valve development from the 'massive' OFT cushion towards the 'hollow' valve leaflets containing the sinus of Valsalva (Henderson 2020). The proximal part of the cushions remains attached to the myocardial border, while the developing leaflets and commissures develop from the distal part of the cushion, that enlarges concomitantly with the expanding arterial wall.

Once the condensed mesenchyme begins to differentiate into cartilage, the surrounding mesenchyme starts to lose its integrity by degradation of the extracellular matrix. This is evident by focal absence of staining in the alcian blue preparations. In Ferguson stage 20 the first signs of the developing sinus of Valsalva are apparent in the septal cushion followed by the appearance of endocardial strands invading the septal cushion from both aortic sides. We could not establish whether the endothelial strands are sprouting from the endothelium of the sinus or arise *de novo* from the mesenchyme of the septal cushion. By stage 21 the endothelial strands have met end-to-end to form a tunnel in the septal cushion penetrating the advancing IA. In stage 24 the tunnel through the septal cushion in *Caiman* has reached an estimated diameter of about 5-10% of the systemic aorta. We have to realize that the main intracardiac communication, the oval foramen between right and left atrium, is far greater allowing much more blood shunting from right to left before hatching. With respect to the pre-hatching amounts of blood involved we assume that the physiological function of the FOP is restricted and maybe even negligible. During the adult cardiac cycle the net flow through the FOP is also very small to non-existent [16] as the left ventricular pressure in the systemic aorta surmounts the pressure in the visceral aorta. The attributed functions of the FOP have been associated to many activities including diving or pH-related postprandial metabolism. The functions [18, 61] require also the contraction of specialized muscle nodules

Preprints (www.preprints.org) | NOT PEER-REVIEWED | Posted: 6 August 2021 doi:10.20944/preprints202108.0157.v1

(dubbed “cogteeth” or “cogwheel” [62, 63]) in the right ventricular outflow to increase right ventricular blood pressure over a threshold to allow the mechanism of opening (and closure) of the foramen by the guarding septal valve leaflet in the systemic aorta [64].

Intriguingly, the cartilage prongs discussed above are spatially associated with the FOP and the ostium of the systemic aorta, but less with that of the visceral aorta. It is tempting to propose a mechanical function in maintaining the size of both these conduits when the open FOP allows right ventricular blood into the systemic aorta.

Preprints (www.preprints.org) | NOT PEER-REVIEWED | Posted: 6 August 2021 doi:10.20944/preprints202108.0157.v1

Material and Methods

The *Caiman latirostris* eggs were donated by René Hedegaard, Krokodille Zoo, Denmark. These were incubated until the desired stage, fixed in formalin at 4°C overnight dehydrated through a graded methanol series and stored in 100% methanol at -20°C. The *Alligator mississipiensis* embryos were obtained through a project from Mark Ferguson, deposited in the Manchester Museum from the University of Manchester (United Kingdom) and allowed to use for scientific purposes. These were fixed and stored in formalin. Additional *Crocodilus niloticus* eggs were obtained from La Ferme au Crocodile, Pierrelatte (France),incubated until the desired stage and treated the same as the caiman embryos above. The total number of embryos studied were 8 caiman embryos, 14 crocodiles and 7 alligators.

Staging of the embryos of these species occurred by the criteria of M. Ferguson [65]. The thorax containing heart and arterial trunks was excised and routinely dehydrated through ethanol. The tissue was embedded standardly in paraffin, sectioned in 7 µm serial sections, collected on objective slides and stained with hematoxylin-eosin and alcian blue as published [19]. Finally, they were coverslipped using Eukit.

Stained sections were scanned at 40 X and made electronically available with the Philips IMS system through the Dept of Pathology, LUMC Leiden, maintained by dr. J Oosting and B. van den Akker.

References.

1. Hinton RB, Yutzey KE. Heart valve structure and function in development and disease. Annu Rev Physiol. 2011;73:29-46. doi: 10.1146/annurev-physiol-012110-142145.

2.Grewal N, Girdauskas E, DeRuiter M, Goumans MJ, Poelmann RE, Klautz RJM, Gittenberger-de Groot AC. The role of hemodynamics in bicuspid aortopathy: a histopathologic study. . Cardiovasc Pathol. 2019, 41:29-37. doi: 10.1016/j.carpath.2019.03.002

3.Michelena HI, Khanna AD, Mahoney D, Margaryan E, Topilsky Y, Suri RM, Eidem B, Edwards WD, Sundt TM 3rd, Enriquez-Sarano. Incidence of aortic complications in patients with bicuspid aortic valves. JAMA. 2011;306:1104-12. doi: 10.1001/jama.2011.1286.

3a. Martin PS, Kloesel B, Norris RA, Lindsay M, Milan D, Body SC. Embryonic Development of the Bicuspid Aortic Valve.J Cardiovasc Dev Dis. 2015 2:248-272. doi: 10.3390/jcdd2040248.

4.Laforest B, Nemer M. GATA5 interacts with GATA4 and GATA6 in outflow tract development. Dev Biol. 2011;358:368-78. doi: 10.1016/j.ydbio.2011.07.037.

5.Odelin G, Faure E, Coulpier F, Di Bonito M, Bajolle F, Studer M, Avierinos JF, Charnay P, Topilko P, Zaffran S. Krox20 defines a subpopulation of cardiac neural crest cells contributing to arterial valves and bicuspid aortic valve. Development. 2018;145:dev151944. doi: 10.1242/dev.151944.

6.Koenig SN, Bosse KM, Nadorlik HA, Lilly B, Garg V. Evidence of Aortopathy in Mice with Haploinsufficiency of *Notch1* in *Nos3*-Null Background. J Cardiovasc Dev Dis. 2015;2:17-30. doi: 10.3390/jcdd2010017

7.Zhao B , Laura Etter, Robert B Hinton Jr, D Woodrow Benson. BMP and FGF regulatory pathways in semilunar valve precursor cells. Dev Dyn 2007;236:971-80. doi: 10.1002/dvdy.21097.

8.Midgett M, López CS, David L, Maloyan A, Rugonyi S. Increased Hemodynamic Load in Early Embryonic Stages Alters Endocardial to Mesenchymal Transition. Front Physiol. 2017;8:56. doi: 10.3389/fphys.2017.00056

9.Peterson JC, Chughtai M, Wisse LJ, Gittenberger-de Groot AC, Feng Q, Goumans MTH, VanMunsteren JC, Jongbloed MRM, DeRuiter MC. Bicuspid aortic valve formation: *Nos3* mutation leads to abnormal lineage patterning of neural crest cells and the second heart field. Dis Model Mech. 2018;11:dmm034637. doi: 10.1242/dmm.034637.

10.Soto-Navarrete MT, López-Unzu MÁ, Durán AC, Fernández B.Soto-Navarrete MT Embryonic development of bicuspid aortic valves. Prog Cardiovasc Dis. 2020;63:407-418. doi: 10.1016/j.pcad.2020.06.008.

11.Poelmann RE, Gittenberger-de Groot AC. Hemodynamics in Cardiac Development. J Cardiovasc Dev Dis. 2018;5:54. doi: 0.3390/jcdd5040054.

12.Hochstetter F. Die Entwicklung des Blutgefässsystems. In O.Hartwig ed. Handbuch der vergleichenden and experimentellen Entwicklungslehre der Wirbeltiere, Fischer Jena, 1906, pp21-166.

13.Goodrich ES. Note on the Reptilian Heart. J Anat . 1919;53:298-304.

14.Sandrone S, Riva M. Bartolomeo Panizza (1785-1867) J Neurol. 2014;261:1249-50. doi: 10.1007/s00415-013-7028-6.

15.Poelman AC. Note sur le systeme circulatoire des Crocodiliens. Bull Acad Belg 1854;21:67-72

16.Axelsson M, Holm S, Nilsson S. Flow dynamics of the crocodilian heart. Am J Physiol. 1989;256:R875-9. doi: 10.1152/ajpregu.1989.256.4.R875.

17.Malvin GM, Hicks JW, Greene ER. Central vascular flow patterns in the alligator Alligator mississipiensis. Am J Physiol. 1995;269:R1133-9. doi: 10.1152/ajpregu.1995.269.5.R1133.

18.Burggren W, Filogonio R, Wang T Cardiovascular shunting in vertebrates: a practical integration of competing hypotheses. Biol Rev Camb Philos Soc. 2020;95:449-471. doi: 10.1111/brv.12572.

19.Poelmann RE, Gittenberger-de Groot AC, Biermans MWM, Dolfing AI, Jagessar A, van Hattum S, Hoogenboom A, Wisse LJ, Vicente-Steijn R, de Bakker MAG, Vonk FJ, Hirasawa T, Kuratani S, Richardson MK. Outflow tract septation and the aortic arch system in reptiles: lessons for understanding the mammalian heart. Evodevo. 2017;8:9. doi: 10.1186/s13227-017-0072-z.

20.Cook AC, Tran VH, Spicer DE, Rob JMH, Sridharan S, Taylor A, Anderson RH, Jensen B. Sequential segmental analysis of the crocodilian heart. J Anat. 2017;231:484-499. doi: 10.1111/joa.12661.

21.Axelsson M, Fritsche R, Holmgren S, Grove DJ, Nilsson S. Gut blood flow in the estuarine crocodile, Crocodylus porosus. Acta Physiol Scand. 1991;142:509-16. doi: 10.1111/j.1748-1716.1991.tb09187.x.

22.Grandidier A 1872 Description de quelques reptiles nouveaux a Madagascar en 1870. Annales des sciences naturelles, Cinquieme Serie, Zologie et Paleontologie, 1872 ;15 : 1-6.

23.Hekkala E, Shirley MH, Amato G, Austin JD, Charter S, Thorbjarnarson J, Vliet KA, Houck ML, Desalle R, Blum MJ. An ancient icon reveals new mysteries: mummy DNA resurrects a cryptic species within the Nile crocodile. Mol Ecol. 2011;20:4199-215. doi: 10.1111/j.1365-294X.2011.05245.x.

24.Jensen B, Christoffels VM Reptiles as a Model System to Study Heart Development. . Cold Spring Harb Perspect Biol. 2020;12:a037226. doi: 10.1101/cshperspect.a037226.

25. Waldo K, Miyagawa-Tomita S, Kumiski D, Kirby ML. Cardiac neural crest cells provide new insight into septation of the cardiac outflow tract: aortic sac to ventricular septal closure. Dev Biol. 1998;196:129-44. doi: 10.1006/dbio.1998.8860.

26. Bartelings MM, Gittenberger-de Groot AC .The outflow tract of the heart--embryologic and morphologic correlations. Int J Cardiol . 1989 22:289-300. doi: 10.1016/0167-5273(89)90270-2.

27.Kirby ML, Gale TF, Stewart DE. Neural crest cells contribute to normal aorticopulmonary septation. Science. 1983;220:1059-61. doi: 10.1126/science.6844926.

28.Kirby ML, Hutson MR. Factors controlling cardiac neural crest cell migration. Cell Adh Migr. 2010;4:609-21. doi: 10.4161/cam.4.4.13489.

29.Poelmann RE, Mikawa T, Gittenberger-de Groot AC. Neural crest cells in outflow tract septation of the embryonic chicken heart: differentiation and apoptosis. Dev Dyn. 1998;212:373-84. doi: 10.1002/(SICI)1097-0177(199807)212:3<373::AID-AJA5>3.0.CO;2-E.

30.Bergwerff M, Verberne ME, DeRuiter MC, Poelmann RE, Gittenberger-de Groot AC. Neural crest cell contribution to the developing circulatory system: implications for vascular morphology? Circ Res. 1998;82:221-31. doi: 10.1161/01.res.82.2.221

31. Peterson JC, Chughtai M, Wisse LJ, Gittenberger-de Groot AC, Feng Q, Goumans MTH, VanMunsteren JC, Jongbloed MRM, DeRuiter MC. Bicuspid aortic valve formation: *Nos3* mutation leads to abnormal lineage patterning of neural crest cells and the second heart field..Dis Model Mech. 2018 11:dmm034637. doi: 10.1242/dmm.034637.

32.Kodo K, Shibata S, Miyagawa-Tomita S, Ong SG, Takahashi H, Kume T, Okano H, Matsuoka R, Yamagishi H. Regulation of Sema3c and the Interaction between Cardiac Neural Crest and Second Heart Field during Outflow Tract Development. Sci Rep. 2017;7:6771. doi: 10.1038/s41598-017-06964-9.

33.Zhou Z, Wang J, Guo C, Chang W, Zhuang J, Zhu P, Li X. Temporally Distinct Six2-Positive Second Heart Field Progenitors Regulate Mammalian Heart Development and Disease. Cell Rep. 2017;18:1019-1032. doi: 10.1016/j.celrep.2017.01.002

34.Mifflin JJ, Dupuis LE, Alcala NE, Russell LG, Kern CB Intercalated cushion cells within the cardiac outflow tract are derived from the myocardial troponin T type 2 (Tnnt2) Cre lineage. Dev Dyn. 2018247:1005-1017. doi: 10.1002/dvdy.24641.

35.Henderson DJ, Eley L, Chaudhry B. New Concepts in the Development and Malformation of the Arterial Valves. Cardiovasc Dev Dis. 2020;7:38. doi: 10.3390/jcdd7040038.

36. Stefanovic S, Etchevers HC, Zaffran S. Outflow Tract Formation-Embryonic Origins of Conotruncal Congenital Heart Disease. J Cardiovasc Dev Dis. 2021 Apr 9;8(4):42. doi: 10.3390/jcdd8040042.

37.Baardman ME, Zwier MV, Wisse LJ, Gittenberger-de Groot AC, Kerstjens-Frederikse WS, Hofstra RM, Jurdzinski A, Hierck BP, Jongbloed MR, Berger RM, Plösch T, DeRuiter MC. Common arterial trunk and ventricular non-compaction in Lrp2 knockout mice indicate a crucial role of LRP2 in cardiac development. Dis Model Mech. 2016;9:413-25. doi: 10.1242/dmm.022053.

38.Sumida H, Akimoto N, Nakamura H. Distribution of the neural crest cells in the heart of birds: a three dimensional analysis. Anat Embryol (Berl). 1989;180:29-35. doi: 10.1007/BF00321897

39.Conway SJ, Henderson DJ, Copp AJ. Pax3 is required for cardiac neural crest migration in the mouse: evidence from the splotch (Sp2H) mutant. Development. 1997;124:505-14.

40.Azhar M, Al-Sammarriae N, Chakrabarti M, Johnson J, Booth K, Conway S, Mathew S. TGFbeta hyperactivation causes development and progression of calcific aortic valve stenosis. In: abstractbook of the Weinstein 2018 Conference, Nara, Japan.

41.Sawada H, Rateri DL, Moorleghen JJ, Majesky MW, Daugherty A. Smooth Muscle Cells Derived From Second Heart Field and Cardiac Neural Crest Reside in Spatially Distinct Domains in the Media of the Ascending Aorta-Brief Report. Arterioscler Thromb Vasc Biol. 2017;37:1722-1726. doi: 10.1161/ATVBAHA.117.309599

42.Gittenberger-de Groot AC, Peterson JC, Wisse LJ, Roest AAW, Poelmann RE, Bökenkamp R, Elzenga NJ, Hazekamp M, Bartelings MM, Jongbloed MRM, DeRuiter MC. Pulmonary ductal coarctation and left pulmonary artery interruption; pathology and role of neural crest and second heart field during development. PLoS One. 2020;15:e0228478. doi: 10.1371/journal.pone.0228478

43.Bajolle F, Zaffran S, Meilhac SM, Dandonneau M, Chang T, Kelly RG, Buckingham ME. Myocardium at the base of the aorta and pulmonary trunk is prefigured in the outflow tract of the heart and in subdomains of the second heart field. Dev Biol;313:25-34. doi: 10.1016/j.ydbio.2007.09.023.

44.Boot MJ, Gittenberger-De Groot AC, Van Iperen L, Hierck BP, Poelmann RE. Spatiotemporally separated cardiac neural crest subpopulations that target the outflow tract septum and pharyngeal arch arteries. Anat Rec A Discov Mol Cell Evol Biol. 2003;275:1009-18. doi: 10.1002/ar.a.10099.

45.Durán AC, López D, Guerrero A, Mendoza A, Arqué JM, Sans-Coma V. Formation of cartilaginous foci in the central fibrous body of the heart in Syrian hamsters (Mesocricetus auratus). J Anat. 2004;205:219-27. doi: 10.1111/j.0021-8782.2004.00326.x.

46.Egerbacher M, Weber H, Hauer S Bones in the heart skeleton of the otter (Lutra lutra). J Anat. 2000;196:485-91. doi: 10.1046/j.1469-7580.2000.19630485.x

47.Daghash, S.M. and Farghali, H.A.M. The cardiac skeleton of the Egyptian Water buffalo (Bubalus bubalis) Int. J. Adv. Res. Biol. Sci. (2017). 4(5): 1-13 DOI: 10.22192/ijarbs

Erdogan S, Lima M, Pérez W. Anat Sci Int. 2014;89:46-52. Inner ventricular structures and valves of the heart in white rhinoceros (Ceratotherium simum). doi: 10.1007/s12565-013-0199-5. 25.

49.Frink RJ, Merrick B. The sheep heart: coronary and conduction system anatomy with special reference to the presence of an os cordis. . Anat Rec. 1974;179:189-200. doi: 10.1002/ar.1091790204

50.Moittié S, Baiker K, Strong V, Cousins E, White K, Liptovszky M, Redrobe S, Alibhai A, Sturrock CJ, Rutland CS. Discovery of os cordis in the cardiac skeleton of chimpanzees (Pan troglodytes). Sci Rep. 2020;10:9417. doi: 10.1038/s41598-020-66345-7

51.White FN Circulation in the reptilian heart (Caiman sclerops). Anat Rec. 1956;125:417-31. doi: 10.1002/ar.1091250302.

52.Young BA. Cartilago cordis in serpents. Anat Rec. 1994;240:243-7. doi: 10.1002/ar.1092400211

53.López D, Durán AC, de Andrés AV, Guerrero A, Blasco M, Sans-Coma V.Formation of cartilage in the heart of the Spanish terrapin, Mauremys leprosa (Reptilia, Chelonia). J Morphol. 2003;258:97-105. doi: 10.1002/jmor.10134

54.Braz JK, Freitas ML, Magalhães MS, Oliveira MF, Costa MS, Resende NS, Clebis NK, Silva NB, Moura CE. Histology and Immunohistochemistry of the Cardiac Ventricular Structure in the Green Turtle (Chelonia mydas). Anat Histol Embryol. 2016;45:277-84. doi: 10.1111/ahe.12195

55.Grebenik EA, Gafarova ER, Istranov LP, Istranova EV, Ma X, Xu J, Guo W, Atala A, Timashev PS. Mammalian Pericardium-Based Bioprosthetic Materials in Xenotransplantation and Tissue Engineering. Biotechnol J. 2020;15:e1900334. doi: 10.1002/biot.201900334

56.Grewal N, Gittenberger-de Groot AC, Thusen JV, Wisse LJ, Bartelings MM, DeRuiter MC, Klautz RJM, Poelmann RE. The Development of the Ascending Aortic Wall in Tricuspid and Bicuspid Aortic Valve: A Process from Maturation to Degeneration. J Clin Med. 2020;9:908. doi: 10.3390/jcm9040908

57.Peterson JC, Wisse LJ, Wirokromo V, van Herwaarden T, Smits AM, Gittenberger-de Groot AC, Goumans MTH, VanMunsteren JC, Jongbloed MRM, DeRuiter MC. Disturbed nitric oxide signalling gives rise to congenital bicuspid aortic valve and aortopathy. Dis Model Mech. 2020;13(9):dmm044990. doi: 10.1242/dmm.044990

58. Panizza B.(1833): 'Sulla struttura del cuore e sulla circolazione del sangue del *Crocodilus lucius*' *Biblioteca Italiana*, Volume 70, p. 87–91.

59.Eisenberg LM, Markwald RR. Molecular regulation of atrioventricular valvuloseptal morphogenesis. Circ Res. 1995;77:1-6. doi: 10.1161/01.res.77.1.1

60.Person AD, Klewer SE, Runyan RB. Cell biology of cardiac cushion development. Int Rev Cytol. 2005;243:287-335. doi: 10.1016/S0074-7696(05)43005-3.

61.Conner JL, Crossley JL, Elsey R, Nelson D, Wang T, Crossley DA. Does the left aorta provide proton-rich blood to the gut when crocodilians digest a meal? . J Exp Biol. 2019;222:jeb201079. doi: 10.1242/jeb.201079.

62.Franklin CE, Axelsson M. An actively controlled heart valve. Nature. 2000;406:847-8. doi: 10.1038/35022652.

63.Syme DA, Gamperl K, Jones DR. Delayed depolarization of the cog-wheel valve and pulmonary-to-systemic shunting in alligators. J Exp Biol. 2002;205:1843-51.

64.Axelsson M, Franklin C, Löfman C, Nilsson S, Grigg G. Dynamic anatomical study of cardiac shunting in crocodiles using high-resolution angioscopy. J Exp Biol. 1996;199:359-65.

65.Ferguson MWJ. Reproductive biology and embryology of the crocodilians. In: Biology of the reptilia vol 14A Ch 5 (eds Gans C, Billett F, Maderson PFA) 1985. Wiley, NewYork, Chichester, Brisbane, Toronto, Singapore.

Preprints (www.preprints.org) | NOT PEER-REVIEWED | Posted: 6 August 2021 doi:10.20944/preprints202108.0157.v1

Legend to the figures

Fig 1. Ferguson stage 17. HE alcian blue stained serially sectioned embryo. Fig a-n from AV canal to pharyngeal arch arteries. Generally, the endocardial cushions stand out because of the alcian blue staining. **Fig a,** myocardium is spongious with a thin compact outer layer. The inlet septum is the most conspicuous part of the interventricular septum located between the left and right sided part of the undivided common ventricle. **Fig b, c,** the outflow tract septal cushion becomes visible. **Fig d, e,** the folding septum becomes only clear more distally. **Fig f,** pulmonary and aortic parietal OFT cushions become apparent, flanking the pulmonary channel and the yet common aortic channel. **Fig g, magnified in fig f,** in the large centrally located septal cushion two streams of condensed mesenchyme, on the pulmonary side (in red) and the aortic side (in blue). The septal cushion becomes subdivided over the main arterial channels. **Fig h,i,** both streams end separately in a bulbous structure as basis for the AP-septum (*) and IA septum (+). **Fig j, magnified in fig k,** the AP stream meets the ventral myocardial spur (#). **Fig l, magnified in m,** the myocardial spur is part of the ventral myocardium. At this level the AP septum is completed. **Fig n,** pharyngeal arch arteries are separated and the connection to the dorsal aorta is present.

Fig 2. Ferguson stage 19. HE alcian blue stained serially sectioned embryo. Fig a-m from AV canal to OFT. **Fig a**, ventricular myocardial inlet septum attached to the central AV cushions between the left and right ventricle. The myocardium is spongy but for the thin outer compact layer. **Fig b,** More ventrally the interventricular communication is visible, while the left ventricular outflow tract becomes apparent. **Fig c,** muscular folding septum appears as continuation of the inlet septum. The septal OFT cushion is located at the tip of the folding septum. **Fig d,** septal cushion with alcian blue stained condensed mesenchyme. The aortic parietal cushion appears on the other side of the LVOT. **Fig e,** the septal cushion is located between both outflow tracts, while the folding septum has shifted to the right side. **Fig f**, In the RVOT the pulmonary parietal cushion is present and the folding septum including the septal cushion takes up a dorsal position. **Fig g,** the most cranial remnant of the muscular folding septum is indicated (Δ). The adjacent condensed mesenchyme (+) belonging to the interaortic septum has appeared in the septal cushion. **Fig h**, a second element of condensed mesenchyme (*) appears ventral to the disappearing myocardium (Δ). **Fig i**, two streams of condensed mesenchyme as part of the aorto-pulmonary septum (*) and the interaortic

Preprints (www.preprints.org) | NOT PEER-REVIEWED | Posted: 6 August 2021 doi:10.20944/preprints202108.0157.v1

septum (+) separate the septal cushion in three subcushions. **Fig j,** more distally only the AP septum continues and receives myocardium (#) from the ventral wall. **Fig k**, the condensed mesenchyme of the AP septum is not present anymore, but the myocardial component has enlarged (#). The pulmonary trunk, the visceral aorta and the systemic aorta are indicated as are the endocardial cushion components. Only the visceral aorta is still encased in myocardium, but note that the arterial wall of the visceral aorta continues within the myocardial tube (dashed line). Fig l, the visceral and systemic aorta are separated at this level by the AP septum (red line). **Fig m**, here, the AP septum is myocardialized (#).

Fig 3. Ferguson stage 20, Fig a-l from AV-canal to OFT. **Fig a,** both in the septal and aortic parietal cushion cartilage is forming (dark blue) which is less evident more distally **(Fig b)**. **Fig c,** the septal cushion containing condensed mesenchyme has a central position. **Fig d and e**, the septal cushion becomes subdivided by both prongs of condensed mesenchyme, belonging to IA septum (+) and AP septum (*), the remnant of the folding septum is indicated (Δ). **Fig f,** The condensed mesenchyme of the IA septum bridges the gap to the aortic parietal cushion whereby the systemic and visceral aorta become separated at this level. The AP septum now contains 3 elements. Enlargement in **Fig g,** condensed mesenchyme (*), flanked by myocardium of the folding septum (Δ) and the ventral myocardium (#). **Fig h,** both IA and AP septa are fully developed at this level. The arrows indicate the sinus of Valsalva in the systemic and visceral aorta. **Fig i,** The arrow indicates a sinus of Valsalva in the pulmonary trunk. **Fig j, k, l,** illustrate the branching of the arterial tree, including the pulmonary arteries, and the carotid arteries from the systemic aorta. The visceral aorta does not branch further.

Fig. 4 Ferguson stage 21, from AV canal to the arterial tree. **Fig a**, the ventricular septum shows its two parts, the inlet septum attached to the central AV cushions and the more ventro-distally located folding septum. **Fig b, c**, the septal cushion showing already cartilage differentiation (dark blue) located on the tip of the folding septum. **Fig d, e**, the right ventricular outflow tract rotates to the right, displacing the folding septum (Δ) to dorsal. **Fig f, g**, the AP (*) and IA (+) streams of condensed mesenchyme are visible. The sinus of Valsalva (white arrow) and the tunnel of the foramen of Panizza (black arrows) are indicated. **Fig h, i, j,** More distally the AP and IA septa become completed by fusion of the septal cushion with the parietal cushion. **Fig k,** branching of the arterial tree.

Preprints (www.preprints.org) | NOT PEER-REVIEWED | Posted: 6 August 2021 doi:10.20944/preprints202108.0157.v1

Fig 5. Ferguson stage 22, Fig a-i, from AV canals to the arterial tree. **Fig a, b,** septal cushion with cartilage between left and right ventricle. **Fig c,** cartilage differentiation in both the septal and aortic parietal cushion. **Fig d,** enlargement of fig c, the septal cartilage related to the IA septum is located on the left, aortic side of the folding septum. **Fig e, f,** The AP (*), (Δ), (#) and the IA (+) septum are completely visible containing their various elements. The tunnel of the foramen of Panizza is present (black arrows). **Fig g-k,** demonstrate the branching pattern of the arterial tree.

Fig 6. Ferguson stage 24, fig a-l, from AV valves to semilunar valve level. **Fig a, b**, the AV cushions have elongated to form free-edged valve leaflets. **Fig c, d,** folding septum including septal cushion is centrally located between left and right ventricular compartments. Cartilage-rich prongs in both OFT cushions. Note that the parietal cushion now contains two cartilaginous centres. **Fig e, f, g, h**, the tunnel of the foramen of Panizza (p) is shown rounding the septal cartilage and joining the sinus of Valsalva (sV) of both aortae. Note that the cartilage is surrounded by a fibrous capsule. **Fig i,** The AP septum is completed. **Fig j,** the IA septum is completed. **Fig k, l,** coronary ostia (yellow arrows) are found in the parietal wall of the systemic aorta, but not the visceral aorta.

Fig 7. Ferguson stage 25, fig a-i, from AV to semilunar valve leaflets. The myocardium of this specimen is more compact compared to the earlier stages described here. **Fig a, b**, the left and right ventricular compartments are completely septated by the combination of folding septum, inlet septum and mesenchymal septum. **Fig c, d,** the left and right ventricular outflow tracts and the ensuing arterial trunks are separated by the AP septum and the IA septum. The aortic parietal cushion contains two cartilaginous elements. **Fig e, f,** show the narrow tunnel of the foramen of Panizza (arrows) through the IA septum (+). **Fig g,** the IA septum at this level is uninterrupted, with the flanking sinus of Valsalva of the visceral and systemic aorta. **Fig h, i,** Both AP and IA septa are obvious, the lumen of the visceral aorta is very narrow in this specimen.

Fig 8. Alligator embryo older > than F stage 25. HE stained Fig h is in addition alcian blue stained, Fig a-h from AV valves to semilunar valves. **Fig a, b, c, d,** the mesenchymal septum is inserted between the right and left ventricular compartments separating both ventricles. It reaches from the tip of the folding septum near the septal cushion (in Fig a) towards the IA

Preprints (www.preprints.org) | NOT PEER-REVIEWED | Posted: 6 August 2021 doi:10.20944/preprints202108.0157.v1

septum (in Fig d, e). The communication between visceral and systemic aorta is still patent (fig d). **Fig e, f,** here, the IA septum is interrupted by the tunnel of the foramen of Panizza (arrow). **Fig g, h,** Both the AP septum and the IA septum are complete at this level.

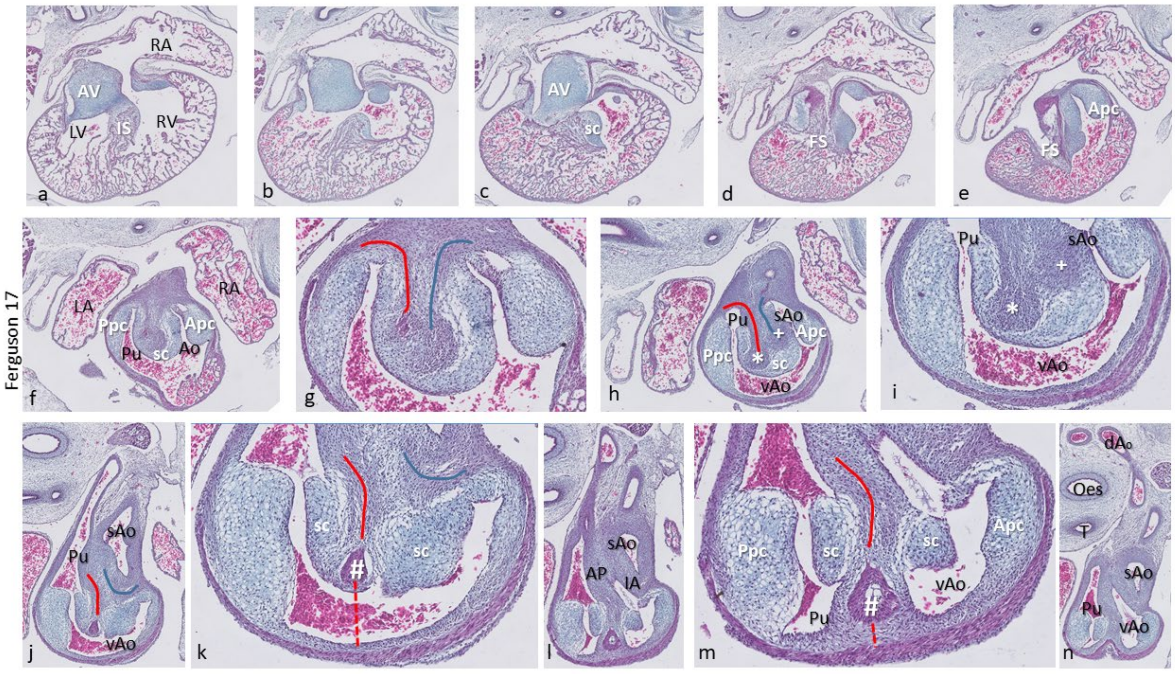

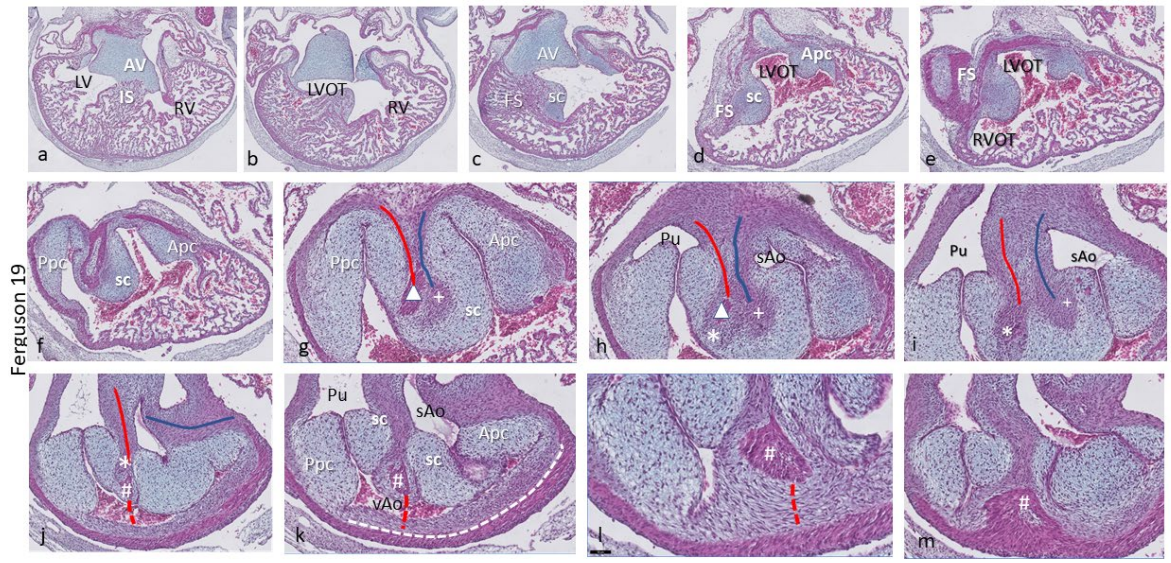

Preprints (www.preprints.org) | NOT PEER-REVIEWED | Posted: 6 August 2021 doi:10.20944/preprints202108.0157.v1

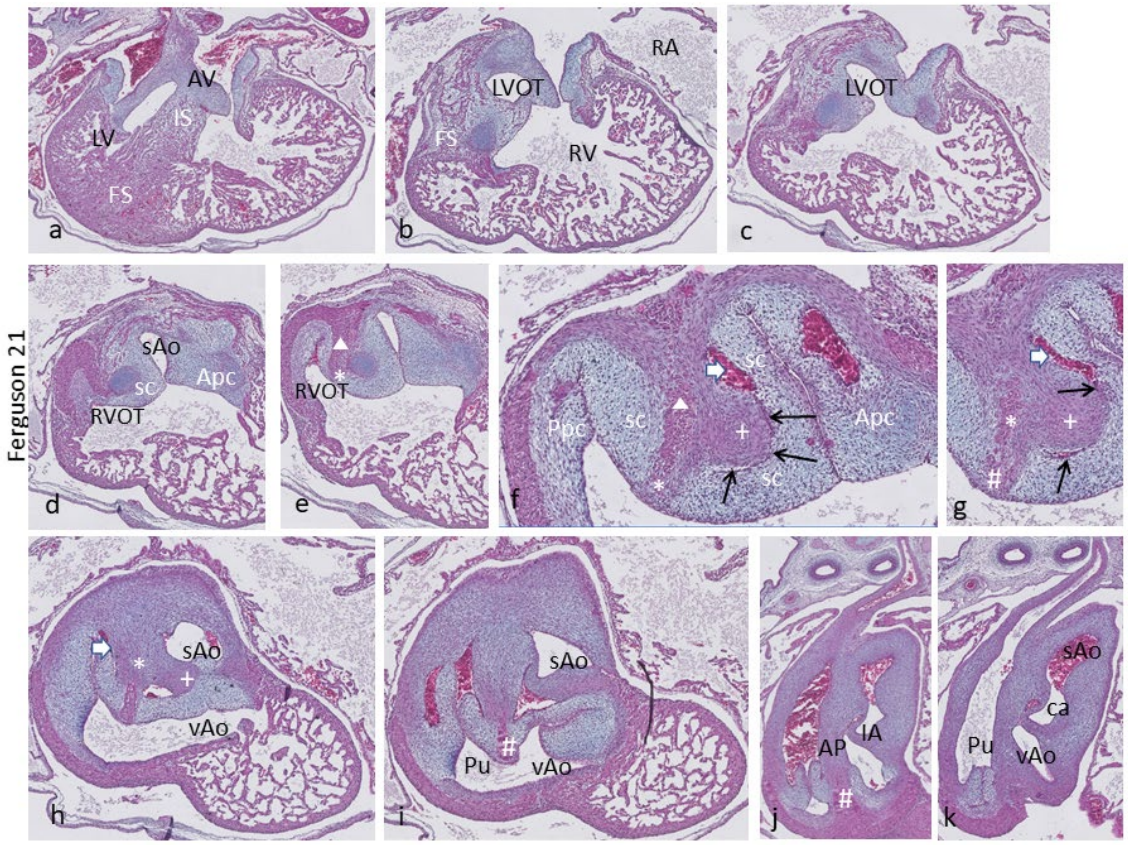

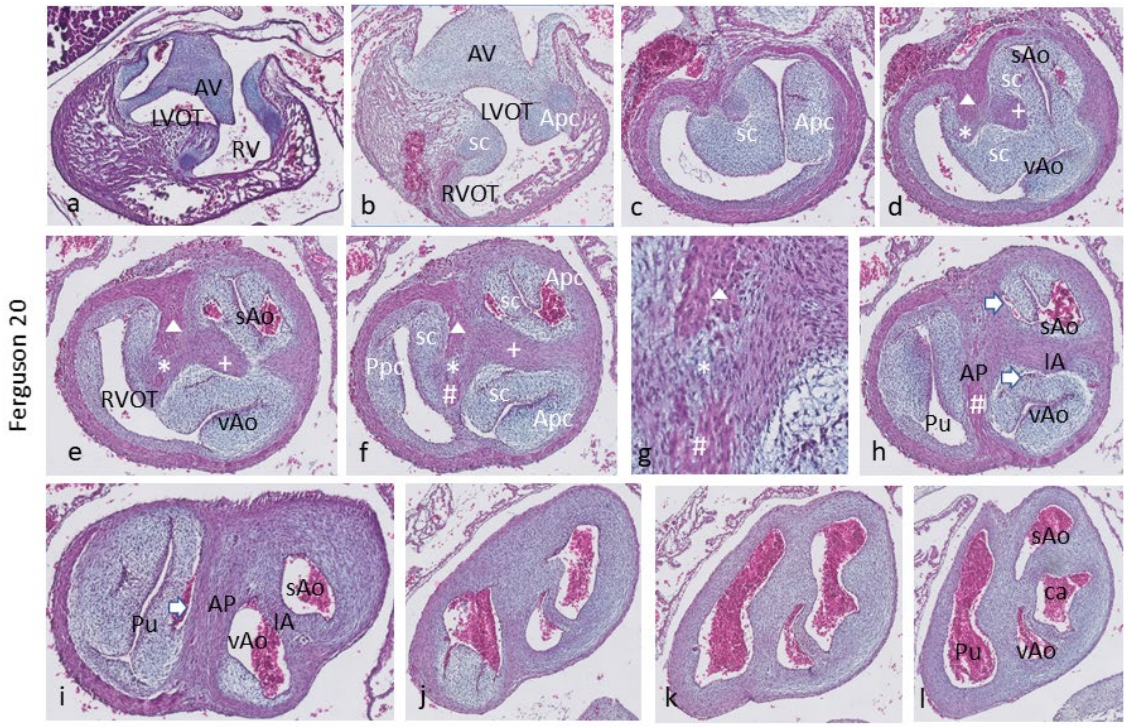

Preprints (www.preprints.org) | NOT PEER-REVIEWED | Posted: 6 August 2021 doi:10.20944/preprints202108.0157.v1

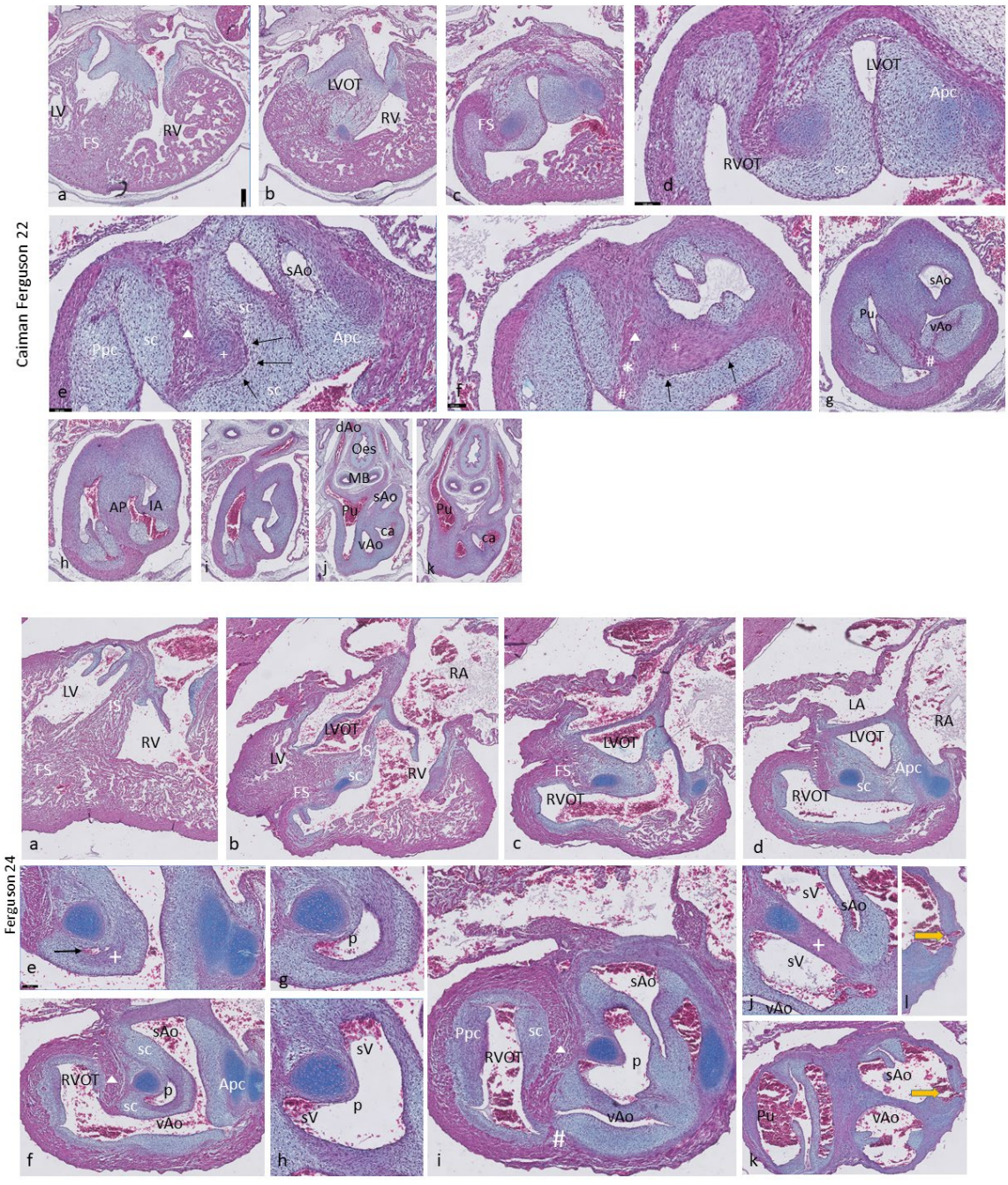

Preprints (www.preprints.org) | NOT PEER-REVIEWED | Posted: 6 August 2021 doi:10.20944/preprints202108.0157.v1